

Short-term forecasting of Italian gas demand

Andrea Marziali^{1,2}, Emanuele Fabbiani², and Giuseppe De Nicolao²

¹Modelling and pricing, A2A

²Department of Electrical, Computer and Biomedical Engineering,
University of Pavia

21st June 2022

Abstract

Forecasting natural gas demand is a key problem for energy providers, as it allows for efficient pipe reservation and power plant allocation, and enables effective price forecasting. We propose a study of Italian gas demand, with particular focus on industrial and thermoelectric components. To the best of our knowledge, this is the first work about these topics. After a preliminary discussion on the characteristics of gas demand, we apply several statistical learning models to perform day-ahead forecasting, including regularized linear models, random forest, support vector regression and neural networks. Moreover, we introduce four simple ensemble models and we compare their performance with the one of basic forecasters. The out-of-sample Mean Absolute Error (MAE) achieved on 2017 by our best ensemble model is 5.16 Millions of Standard Cubic Meters (MSCM), lower than 9.57 MSCM obtained by the predictions issued by SNAM, the Italian Transmission System Operator (TSO).

Keywords— Natural gas; time series forecasting; neural networks; statistical learning; ensemble methods

1 Introduction

Natural gas is one of the most important energy sources in Italy: it feeds domestic and industrial heating, production processes and thermoelectric power plants. Data from SNAM Rete Gas, the Italian Transmission System Operator (TSO), show that, in 2017, Thermoelectric Gas Demand (TGD) accounted for 35.9% of the total consumption, Industrial Gas Demand (IGD) for 22.4% and Residential Gas Demand (RGD) for the remaining 41.7% [1].

Accurate forecasting models for the overall Gas Demand (GD), as well as for its three main components, can help energy providers to improve pipe reservation and stock planning and prevent financial penalties due to network unbalance. Moreover, GD is closely correlated with natural gas price, which is a key input for determining the optimal production plan of thermal power plants.

In this study, we follow and extend a previous work, focusing on RGD [9], in three directions: first, we analyse IGD and TGD, thus allowing for the prediction of the overall Italian gas demand; second, we introduce four more models (lasso, elastic net, random forest and support vector regression); third, we present four ensemble models, i.e. forecasters obtained by the suitable aggregation of first-level forecasts.

The task of forecasting natural gas demand is addressed by an extensive literature, which is reviewed and classified in [16] and [14]. The latter detects four dimensions to classify works: prediction area, prediction horizon, method and inputs. Our work focuses on country-level, day-ahead prediction, adopts statistical learning models and leverages past gas demand, temperature and calendar features as input variables.

Country-wide short-term forecasting of natural gas demand is achieved in [18] using support vector regression with false neighbours filtered. The authors show the superior performance of the method in forecasting UK gas demand with respect to Auto-Regressive Moving Average (ARMA) models and neural networks (ANN). Azadeh et al. [2] propose an adaptive network-based fuzzy inference system (ANFIS) to predict Iranian gas demand, which outperforms classical time series methods and ANN. A more advanced model, combining wavelet transform, genetic algorithm, ANFIS and ANN is applied in [12] to Greek gas distribution network.

To the best of our knowledge, no study focuses on Italian GD and its peculiar features. In [3], gas consumption of two small Italian towns is analysed and the strong dependence of gas demand on weather is highlighted. Such a relation is reported also in other countries [5, 13].

The contribution of this paper is threefold: first, we present the statistical properties of Italian RGD, IGD and TGD; second, we develop and compare several different machine-learning models; third, we discuss the improvement obtained by introducing basic ensemble methods.

The paper is organised as follows. In Section 2 we present the task and the available data, while in Section 3 we describe the most relevant features of IGD and TGD. After discussing feature engineering (Section 4), in Section 5 we

provide a quick overview of adopted models. Training and hyperparameter tuning are presented in Section 6, results are discussed in Section 7, while Section 8 discusses future developments and concludes the paper.

2 Problem statement

Three tasks are addressed in this paper, all of them concerning Italian gas demand: (i) day-ahead forecasting of daily Industrial Gas Demand (IGD), (ii) the same for the Thermoelectric Gas Demand (TGD), and (iii) the composition of IGD, TGD and Residential Gas Demand (RGD) forecasts to predict the overall Italian Gas Demand (GD).

IGD includes demand by industrial plants and large commercial buildings (e.g. shopping centres), while TGD only accounts for the fuel required by thermoelectric power plants.

Although other minor components of GD exist, in this study it is assumed that, in any day t :

$$GD(t) = IGD(t) + TGD(t) + RGD(t)$$

The datasets for both TGD and IGD are 12 years long, ranging from 2007 to 2018, and made of 3 fields: date (t), forecasted average temperature in Northern Italy (T)¹, and gas demand (either IGD or TGD).

RGD, IGD, TGD and the overall GD are shown in Fig. 1.

¹weather forecast were provided by Meteologica, an Italian specialized company

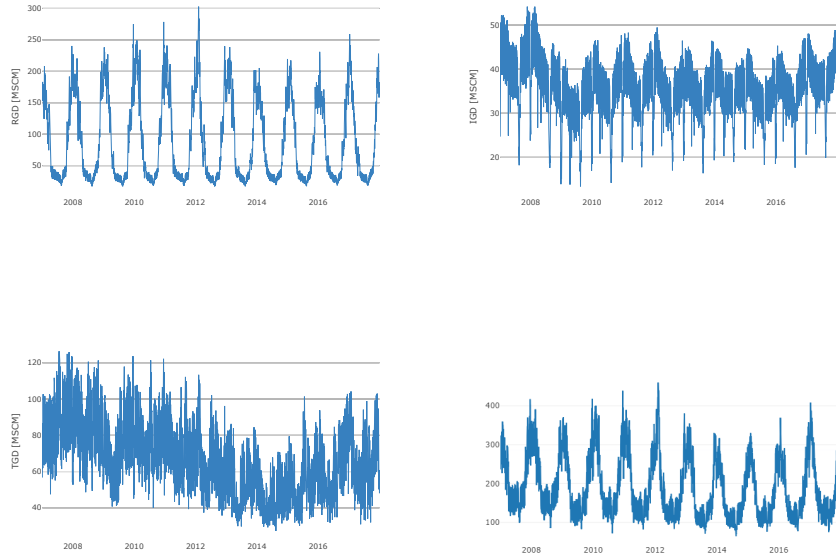


Figure 1: Top row, left panel: Italian Residential Gas Demand (RGD), right panel: Italian Industrial Gas Demand (IGD); bottom row, left panel: Italian Thermoelectric Gas Demand (TGD), right panel: overall Italian Gas Demand (TGD)

3 Exploratory analysis

3.1 Industrial gas demand

Industrial Gas Demand (IGD) does not exhibit strong trends from 2007 to 2018: a significant decrease is only recorded in 2009, following the financial crisis started in the previous year.

The series presents consistent weekly and yearly seasonal patterns. As most of the industrial facilities stop or slow down production during the weekend, IGD is lower on Saturdays and Sundays. In August and at the end of December, traditional holiday periods in Italy, IGD drops to about half of its average value. Other holidays, such as Easter and the Labour Day, result in similar effects, although more limited in time.

During the year, IGD shows a decreasing trend from January to August and an increasing one from September to December, due to the effect of temperature: colder weather during the winter calls for greater gas consumption for environmental heating.

Such features are clearly shown in Fig. 2, where 11 years of IDG are superimposed, aligning weekdays to better represent periodic behaviours.

The periodogram in Fig. 3 presents peaks at periods 365.25 and 7, caused by yearly and weekly seasonality, respectively, while other relevant values are ascribable to multiple harmonics of the fundamental ones. Notably, the magnitude of the weekly component is greater than the ones relative to yearly seasonality, a significant difference from what shown for RGD [9].

Previous studies proved that temperature is one of the most important exogenous variables which affect gas demand [9, 14, 3, 5]: however, the relation is intuitively stronger in the case of RGD, being natural gas a widespread fuel for domestic heating. It is also worth considering the so-called Heating Day Degrees (HDD) that are defined as $HDD = \max(18 - T, 0)$, where T is the temperature in degrees Celsius. The correlation coefficients, computed on the entire dataset, between IGD and temperature and between IGD and HDD are -0.34 and 0.28 respectively, see Fig. 4 for the scatter plots.

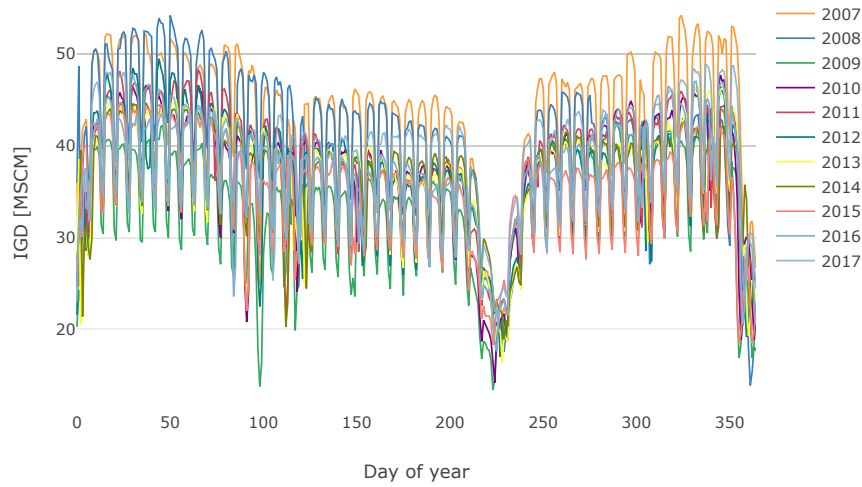


Figure 2: IGD, years 2007-2017: the time series is shifted to align weekdays

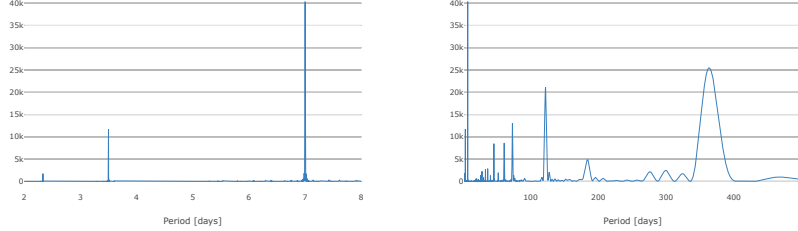


Figure 3: IGD periodogram. Left panel: periods from 0 to 8 days; right panel: periods from 0 to 500 days

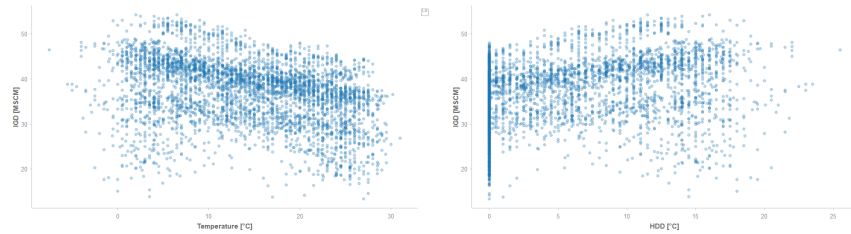


Figure 4: Effect of temperature on IGD. Left panel: IGD vs temperature; right panel: IGD vs HDD

3.2 Thermoelectric gas demand

Differently from IGD, Thermoelectric Gas Demand (TGD) shows a clear trend over years - see ???. From 2008 to 2014 the long-term drift is decreasing, mostly due to the growing importance of renewable sources of electric power, while, since 2014, it is almost constant, due to the decrease in subsidies to the installation of photovoltaic systems.

Moreover, TGD shows a greater variance with respect to IGD and RGD, as the year-over-year plot shows - Fig. 5. TGD is indeed influenced by several different factors, including prices of electric power, gas and European Emission Allowance (EUA) certificates, which exhibit a large volatility [17]. This feature explains why yearly periodicity is relatively less important in TGD than in IGD and RGD. As periodograms in Fig. 6 show, the most relevant spectral components are located at a period of 7 days, which is coherent with Italian power demand [6].

The similarity in features between TGD and power demand appears also when investigating the relation with temperature, see Fig. 7. TGD increases as weather gets colder, but also as it gets hotter: during the summer air conditioning pushes the demand for electric power and more thermoelectric production

is required. In order to capture this pattern, we define the Heating and Cooling Day Degrees (HCDD). Let T be the temperature in Degrees Celsius:

$$\text{HCDD} = |T_c - T|$$

We found that $T_c = 16^\circ\text{C}$ maximises the linear correlation with TGD. The correlation coefficient between HCDD and TGD is 0.28, higher than 0.15 found between TGD and HDD and -0.08 found between TGD and temperature.

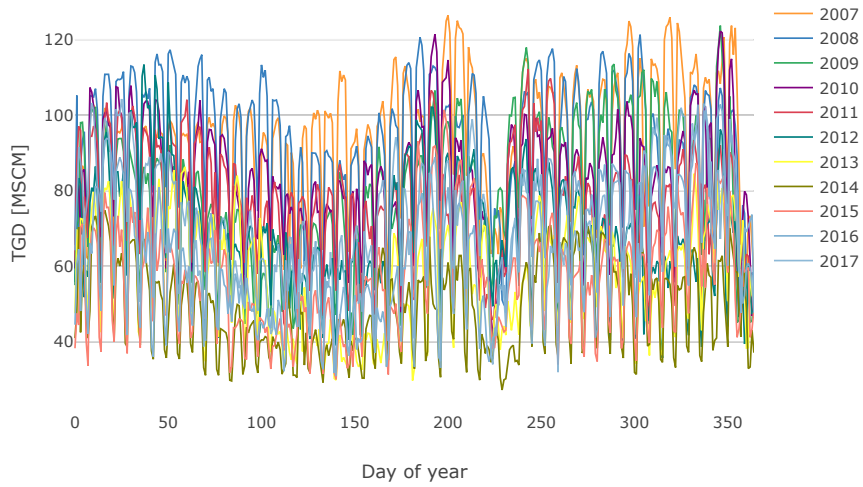


Figure 5: TGD, years 2007-2017: the time series is shifted to align weekdays

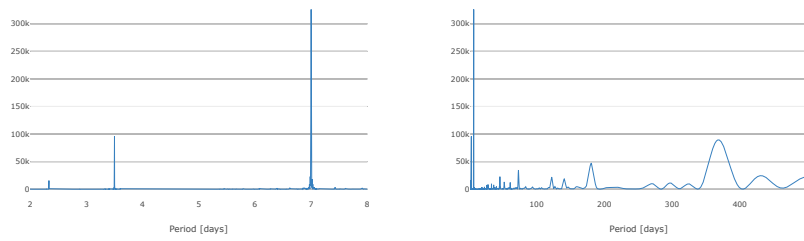


Figure 6: TGD periodogram. Left panel: periods from 0 to 8 days; right panel: periods from 0 to 500 days

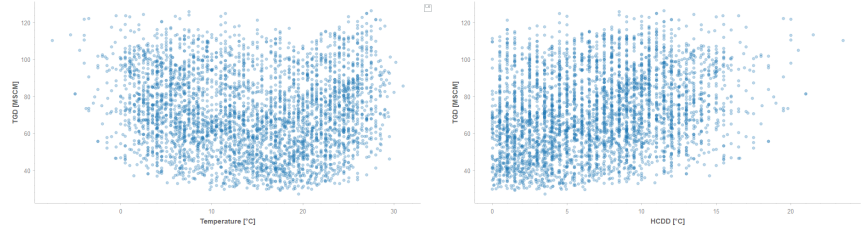


Figure 7: Effect of temperature on TGD. Left panel: TGD vs temperature; right panel: TGD vs HCDD

4 Feature extraction

Following the highlights presented in the previous section, we augmented the dataset for both series with autoregressive terms, calendar features, temperature and its derived variables. Where not stated otherwise, the following processing steps were performed on both IGD and TGD datasets.

In order to capture the yearly periodicity and the concurrent effect of holidays, it is convenient to recall the notion of similar day [9].

Let the following definitions hold, where t and τ are used to identify calendar dates:

- $\text{year}(t)$ is the year to which day t belongs;
- $\text{weekday}(t)$ is the weekday of day t , e.g. Monday, Tuesday, etc;
- $\text{yearday}(t)$ is the day number within $\text{year}(t)$ starting from January 1, whose *yearday* is equal to 1.

Definition 1 (Similar Day). *If t is not a holiday², its similar day $\tau^* = \text{sim}(t)$ is*

$$\tau^* = \arg \min_{\tau} |\text{yearday}(\tau) - \text{yearday}(t)|$$

subject to

- $\text{year}(\tau) = \text{year}(t) - 1$;
- $\text{weekday}(\tau) = \text{weekday}(t)$;
- τ is not a holiday.

If t is a holiday, its similar day $\tau^ = \text{sim}(t)$ is the same holiday in the previous year.*

²According to the Italian calendar, holidays are: 1 January, 6 January, 25 April, 1 May, 2 June, 15 August, 1 November, 8, 25 and 26 December, Easter and Easter Monday.

Feature	Reference time	Type	Series
Gas demand series	$t-1$	continuous	RGD, IGD, TGD
Gas demand series	$t-7$	continuous	RGD, IGD, TGD
Gas demand series	$\text{sim}(t)$	continuous	RGD, IGD, TGD
Gas demand series	$\text{sim}(t-1)$	continuous	RGD, IGD, TGD
Forecasted temperature	t	continuous	RGD, IGD, TGD
Forecasted temperature	$t-1$	continuous	RGD, IGD, TGD
Forecasted temperature	$t-7$	continuous	RGD, IGD, TGD
Forecasted temperature	$\text{sim}(t)$	continuous	RGD, IGD, TGD
Forecasted HDD	t	continuous	RGD, IGD
Forecasted HDD	$t-1$	continuous	RGD, IGD
Forecasted HDD	$t-7$	continuous	RGD, IGD
Forecasted HDD	$\text{sim}(t)$	continuous	RGD, IGD
Forecasted HCDD	t	continuous	TGD
Forecasted HCDD	$t-1$	continuous	TGD
Forecasted HCDD	$t-7$	continuous	TGD
Forecasted HCDD	$\text{sim}(t)$	continuous	TGD
Weekday	t	categorical	RGD, IGD, TGD
Holiday	t	dummy	RGD, IGD, TGD
Day after holiday	t	dummy	RGD, IGD, TGD
Bridge holiday	t	dummy	RGD, IGD, TGD

Table 1: Features

To predict a series at time t , we selected its samples at times $t-1$, $t-7$, $\text{sim}(t)$ and $\text{sim}(t-1)$. The last was introduced because the difference between values at times $\text{sim}(t)$ and $\text{sim}(t-1)$ was found to be a good proxy of the difference between targets at times t and $t-1$.

As calendar features, we introduced dummy variables to account for weekdays and binary variables for holidays. Binary variables were also added to identify: (i) bridges, i.e. working days preceded and followed by either Saturdays, Sundays or holidays, and (ii) days after holidays, i.e. working days which immediately follow an holiday and are not bridges.

We selected as inputs also forecasted temperatures at times t , $t-1$, $t-7$ and $\text{sim}(t)$, while we neglected $\text{sim}(t-1)$, as hints about the value at time t are not needed. In view of what shown in Section 3, for IGD, also HDD at the same times were introduced, while, for TGD, HCDD took the place of HDD.

Table 1 reports the complete list of features.

5 Predictive models

We selected nine basic models, which can be grouped into three categories:

- regularized linear models: ridge regression, lasso and elastic net

- non-linear models: Torus model [6], support vector regression, random forest, neural networks
- non-parametric models: Gaussian Process, nearest neighbour

Five of them, namely ridge regression, Gaussian Process (GP), Torus model, nearest neighbours and neural networks, were already applied to RGD: we thus refer to [9] for their description.

Moreover, we introduced four ensemble models, described in Section 5.2, which aggregate forecasts issued by a subset of the basic models:

- simple average
- average on an optimized subset of basic forecasts (subset average)
- weighted average
- support vector regression.

5.1 Basic models

Regularized linear models

Ridge regression, lasso and elastic net [7] are methods to identify the parameter vector $\beta \in \mathbb{R}^p$ of a model \hat{f} in the form:

$$\hat{f}(\mathbf{X}) = \mathbf{X}\beta, \quad \beta \in \mathbb{R}^p \quad (1)$$

being $\mathbf{X} \in \mathbb{R}^{n \times p}$ the regression matrix, whose dimensions are the number of samples n and features p .

To prevent overfitting and improve generalization capabilities, they include in the loss function a penalty on the magnitude of β :

$$\begin{aligned} \beta^{\text{ridge}} &:= \arg \min_{\beta} \|\mathbf{y} - \mathbf{X}\beta\|^2 + \lambda \|\beta\|^2 \\ \beta^{\text{lasso}} &:= \arg \min_{\beta} \|\mathbf{y} - \mathbf{X}\beta\|^2 + \lambda \|\beta\| \\ \beta^{\text{elastic net}} &:= \arg \min_{\beta} \|\mathbf{y} - \mathbf{X}\beta\|^2 + \lambda (\alpha \|\beta\|^2 + (1 - \alpha) \|\beta\|) \end{aligned}$$

Different penalties result in specific shrinking patterns: in ridge regression, parameters are all shrunk towards zero, while in the lasso the least relevant ones are set equal to zero, and in the elastic net an intermediate effect is achieved.

Both λ and α play the role of hyperparameters: λ controls the strength of the parameter shrinkage, while α the balance between penalties on the norm and the squared norm of β .

Support vector regression

Linear support vector regression (SVR) is also a method to find the β parameter vector of Eq. (1):

$$\beta^{\text{svr}} := \arg \min_{\beta} \frac{1}{2} \|\beta\|^2 + c \sum_{i=1}^n L_\epsilon(y_i, \mathbf{x}_i \cdot \beta) \quad (2)$$

where y_i denotes the i -th element of the target vector $\mathbf{y} \in \mathbb{R}^n$, \mathbf{x}_i the i -th row of the feature matrix $\mathbf{X} \in \mathbb{R}^{n \times p}$ and L_ϵ is an ϵ -insensitive loss function:

$$L_\epsilon(y, \hat{y}) := \begin{cases} 0 & |y - \hat{y}| < \epsilon \\ |y - \hat{y}| - \epsilon & \text{otherwise} \end{cases}$$

The hyperparameters are the real-valued constants c and ϵ .

It is possible to show that the input data only enter the optimization problem for β^{svr} in the dot product $\mathbf{x}_i \cdot \mathbf{x}_j$, where \mathbf{x}_i and \mathbf{x}_j are rows of the input matrix \mathbf{X} [15]. The dot product can be replaced by a function $\kappa(\mathbf{x}_i, \mathbf{x}_j)$, called kernel, under suitable assumptions on κ [4], making the SVR model non-linear. In the following, with "SVR" we will refer to non-linear SVR.

Random forest

Random forest is based on Classification and Regression Trees (CART) [10]. CARTs perform a recursive feature-wise partitioning of the input space and fit local linear regressions on each region of the final partition. CARTs are known to be unstable and prone to overfitting: in order to overcome these limitations, random forest models grow multiple CARTs, resorting to so-called data and feature bagging. Bagging or bootstrap aggregating is a random selection of a subset of a dataset, that is repeated multiple times (with replacement). Models are then trained on each subset. By applying bagging to both data and features, each tree gets trained on different samples and feature sets. Forecasts performed by all models are then averaged to get the final prediction, leading to an overall stable model.

5.2 Ensemble models

Aggregation, also known as blending, has been proven to be an effective technique to improve overall accuracy and stability [11, 8]. Four alternative methods to aggregate forecasts of basic models were considered.

The most trivial aggregation is the arithmetic average of the forecasts achieved by basic models. Given a test input \mathbf{x}^* , and M basic forecasts $\hat{f}_i(\mathbf{x}^*)$, $i = 1, \dots, M$, the ensemble forecast $\hat{f}_*(\mathbf{x}^*)$ is:

$$\hat{f}_*(\mathbf{x}^*) = \frac{1}{M} \sum_{i=1}^M \hat{f}_i(\mathbf{x}^*)$$

A second choice is the weighted average of basic forecasts:

$$\begin{cases} \hat{f}_*(\mathbf{x}^*) = \sum_{i=1}^M w_i \hat{f}_i(\mathbf{x}^*) \\ w_i \geq 0 \\ \sum_{i=1}^M w_i = 1 \end{cases}$$

The weights w_i are obtained by minimising the sum of squared residuals between the ensemble forecast and the target vector on a suitable dataset.

A third choice is an average on a subset of $\bar{M} < M$ basic forecasts, \bar{M} being an additional hyperparameter. The subset is determined by comparing iteratively the two forecasts with the higher correlation and keeping the one achieving the lowest Mean Absolute Error (MAE), until only \bar{M} basic forecasts remain.

The fourth ensemble method consists in fitting a SVR model using basic forecasts as features.

6 Experiments

In order to train both basic and ensemble models, we partitioned the dataset into three subsets: the training set was used to train basic models, the validation one to train ensemble models, and the test set to assess out-of-sample performances. For the sake of robustness, we used five one-year long test sets ranging from 2014 to 2018. For each test set, the validation set covers the previous year, while the training set includes all samples before the start of the validation set. For instance, considering 2017 as test set, the validation set covers 2016, while the training set ranges from 2007 to 2015. Note that the basic models that were compared to ensemble ones were trained on the union of the validation and training data. This was done in order to avoid any bias in favour of ensemble models that leverage on information from both training and validation sets.

Hyperparameters of the Torus model were tuned by maximising AIC, those of the Gaussian Process by maximising the marginal likelihood, while for all the other basic models a five-fold cross validation on the training set was performed.

Out-of-sample performances were evaluated in terms of Mean Absolute Error (MAE):

$$\text{MAE} = \frac{1}{n} \sum_{i=1}^n |y - \hat{y}|$$

where y and \hat{y} are the actual value and its forecast, while n is the number of samples in the considered test set. MAE was preferred over percent or relative error metrics due to the large range of values assumed by the target variable, which would give undue importance to poor performances during low-demand periods.

Model	2014	2015	2016	2017	2018	Average
Ridge	3,15	3,30	3,06	2,95	3,55	3,20
Lasso	3,16	3,30	3,06	2,95	3,56	3,20
Elastic net	3,16	3,30	3,06	2,95	3,56	3,20
SVR	2,78	2,85	2,62	2,38	2,93	2,71
GP	2,46	2,68	2,58	2,57	2,83	2,63
KNN	5,77	4,67	5,46	5,05	5,65	5,32
Random forest	3,56	3,08	3,33	3,46	3,55	3,39
Torus	2,37	3,18	2,66	2,54	3,28	2,81
ANN	2,58	2,76	2,68	2,43	3,10	2,71
Simple average	2,58	2,65	2,56	2,45	2,90	2,63
Subset average	2,24	2,69	2,16	2,09	2,56	2,35
Weighted average	2,17	2,59	2,34	2,06	2,64	2,35
SVR aggregation	2,10	2,59	2,30	2,19	2,64	2,36

Table 2: Out-of-sample MAEs on RGD. Best performers over each year are in boldface; the average of yearly MAEs for each model is reported in the last column

7 Results

Mean absolute errors for RGD, IGD and TGD are reported, respectively, in Table 2, Table 3 and Table 4, while Table 5 summarizes average performance across all test sets and provides MAE on the overall Italian gas demand.

Ensemble models consistently outperform basic ones: in particular, weighted average achieves the best average MAE on each series. A possible explanation of this resides in the fact that different models are better at capturing specific relations: in [9], for instance, it was shown that ANN achieves the best results in winter, while GP in summer, suggesting that the former are better at modelling the impact of weather, while the latter can better follow seasonal patterns. Aggregation can mitigate errors committed by single models, thus increasing the overall accuracy. The improvement in performance due to aggregation is particularly evident in RGD, where the best basic model is outperformed by the best ensemble model by 0.27 Millions of Standard Cubic Meters (MSCM), while the gap is reduced to 0.04 MSCM on both IGD and TGD.

For what concern basic models, GP, ANN and SVR achieve the best average MAE across all the series, with differences between each other smaller than 0.11 MSCM. Notably, results achieved by such models are also stable over different test sets. On the other hand, KNN is consistently the worst performer, due to its poor capability of modelling influence of temperature and holidays.

Finally, analyzing the results on the overall gas demand, we notice that the gap between the best basic and ensemble models is narrower with respect to single series: 0.19 MSCM, while it is 0.27 for RGD.

Model	2014	2015	2016	2017	2018	Average
Ridge	0,71	0,75	0,75	0,74	0,77	0,75
Lasso	0,71	0,75	0,75	0,74	0,77	0,75
Elastic Net	0,71	0,75	0,75	0,74	0,77	0,75
SVR	0,58	0,57	0,58	0,7	0,75	0,64
GP	0,58	0,61	0,61	0,68	0,70	0,64
KNN	1,16	1,49	1,25	1,95	1,23	1,42
Random Forest	0,72	0,74	0,82	1,02	0,84	0,83
Torus	0,94	0,96	0,97	1,05	1,10	1,00
ANN	0,62	0,66	0,80	0,57	0,74	0,68
Simple average	0,57	0,60	0,62	0,69	0,66	0,63
Subset average	0,58	0,61	0,63	0,66	0,67	0,63
Weighted average	0,54	0,54	0,55	0,67	0,70	0,60
SVR aggregation	0,55	0,56	0,77	0,57	0,80	0,65

Table 3: Out-of-sample MAEs on IGD. Best performers over each year are in boldface; the average of yearly MAEs for each model is reported in the last column

Model	2014	2015	2016	2017	2018	Average
Ridge	3,70	3,73	4,15	4,26	4,48	4,06
Lasso	3,70	3,73	4,15	4,26	4,49	4,07
Elastic Net	3,70	3,73	4,15	4,26	4,49	4,07
SVR	3,19	3,40	3,64	4,33	4,33	3,78
GP	3,53	3,49	3,70	4,39	4,34	3,89
KNN	4,83	6,13	5,22	5,83	5,54	5,51
Random Forest	4,29	4,79	4,73	5,00	4,78	4,72
Torus	3,41	3,98	4,48	4,96	4,94	4,35
ANN	3,19	3,40	3,97	4,32	4,41	3,86
Simple average	3,10	3,52	3,77	4,22	4,35	3,79
Subset average	3,12	3,34	3,76	4,27	4,35	3,77
Weighted average	3,02	3,34	3,72	4,29	4,31	3,74
SVR aggregation	3,25	3,34	3,66	4,27	4,35	3,78

Table 4: Out-of-sample MAEs on TGD. Best performers over each year are in boldface; the average of yearly MAEs for each model is reported in the last column

Model	Residential	Industrial	Thermoelectric	Italian
Ridge	3,20	0,75	4,06	6,13
Lasso	3,20	0,75	4,07	6,13
Elastic Net	3,20	0,75	4,07	6,13
SVR	2,71	0,64	3,78	5,34
GP	2,63	0,64	3,89	5,45
KNN	5,32	1,42	5,51	9,42
Random Forest	3,39	0,83	4,72	6,85
Torus	2,81	1,00	4,35	6,37
ANN	2,71	0,68	3,86	5,47
Simple average	2,63	0,63	3,79	5,49
Subset average	2,35	0,63	3,77	5,2
Weighted average	2,35	0,60	3,74	6,11
SVR aggregation	2,36	0,65	3,78	5,15

Table 5: Averages of the yearly MAE on Residential (RGD), Industial (IGD), Thermoelectric (TGD) and global Italian gas demand

8 Conclusions

We analyzed industrial and thermoelectric components of the Italian daily gas demand, complementing a previous study concerning residential demand, and we compared several forecasting models on the three series. We showed how industrial and thermoelectric demand show different relations with temperature, and intuitive ways to craft features to properly take them into account, thus paving the way to further studies on the topic. We introduced four simple ensemble models, in addition to nine statistical learning models, and we provided a comparison of their performances. We found aggregated models to be consistently more effective than basic ones. To the best of our knowledge, the only benchmark available for the task is represented by the forecasts issued by SNAM Rete Gas, the Italian Transmission System Operator (TSO). The out-of-sample Mean Absolute Error (MAE) achieved on 2017 by our beat model is 5.16 MSCM, while SNAM predictions result in a MAE of 9.57 MSCM. Comparison over previous periods is not meaningful, as SNAM introduced an improved model at the beginning of 2017. Future works can thus take our study as a baseline to experiment more complex models to predict Italian gas demand and its main components.

References

- [1] Italian natural gas demand report. <http://pianodecennale.snamretegas.it/it/domanda-offerta-di-gas-in-italia/domanda-di-gas-naturale.html>. Accessed: 2019-01-31.
- [2] A Azadeh, SM Asadzadeh, and A Ghanbari. An adaptive network-based fuzzy inference system for short-term natural gas demand estimation: uncertain and complex environments. *Energy Policy*, 38(3):1529–1536, 2010.

- [3] Lorenzo Baldacci, Matteo Golfarelli, Davide Lombardi, and Franco Sami. Natural gas consumption forecasting for anomaly detection. *Expert Systems with Applications*, 62:190 – 201, 2016.
- [4] Theodoros Evgeniou, Massimiliano Pontil, and Tomaso Poggio. Regularization networks and support vector machines. *Advances in computational mathematics*, 13(1):1, 2000.
- [5] Salvador Gil and J Deferrari. Generalized model of prediction of natural gas consumption. *Journal of energy resources technology*, 126(2):90–98, 2004.
- [6] Alice Guerini and Giuseppe De Nicolao. Long-term electric load forecasting: A torus-based approach. In *2015 European Control Conference (ECC)*, pages 2768–2773, July 2015.
- [7] T. Hastie, R. Tibshirani, and J. Friedman. *The Elements of Statistical Learning: Data Mining, Inference, and Prediction, Second Edition*. Springer Series in Statistics. Springer New York, 2009.
- [8] Andrzej Janusz. Combining multiple classification or regression models using genetic algorithms. In Marcin Szczuka, Marzena Kryszkiewicz, Sheela Ramanna, Richard Jensen, and Qinghua Hu, editors, *Rough Sets and Current Trends in Computing*, pages 130–137, Berlin, Heidelberg, 2010. Springer Berlin Heidelberg.
- [9] Andrea Marzali, Emanuele Fabbiani, and Giuseppe De Nicolao. Italian residential gas demand forecasting. *xxx*, xxx(xxx):xxx, 2019.
- [10] K.P. Murphy and F. Bach. *Machine Learning: A Probabilistic Perspective*. Adaptive Computation and Machi. MIT Press, 2012.
- [11] D. Opitz and R. Maclin. Popular ensemble methods: An empirical study. *Journal of Artificial Intelligence Research*, 11:169–198, aug 1999.
- [12] Ioannis P Panapakidis and Athanasios S Dagoumas. Day-ahead natural gas demand forecasting based on the combination of wavelet transform and anfis/genetic algorithm/neural network model. *Energy*, 118:231–245, 2017.
- [13] H Sarak and A Satman. The degree-day method to estimate the residential heating natural gas consumption in turkey: a case study. *Energy*, 28(9):929 – 939, 2003.
- [14] Dario Šebalj, Josip Mesarić, and Davor Dujak. Predicting natural gas consumption—a literature review. In *28th International Conference "Central European Conference on Information and Intelligent Systems"*, 2017.
- [15] Alex J. Smola and Bernhard Schölkopf. A tutorial on support vector regression. *Statistics and Computing*, 14(3):199–222, Aug 2004.
- [16] Božidar Soldo. Forecasting natural gas consumption. *Applied Energy*, 92:26–37, 2012.

- [17] Rafal Weron. *Modeling and Forecasting Electricity Loads and Prices: A Statistical Approach*. Number hsbook0601 in HSC Books. Hugo Steinhaus Center, Wroclaw University of Technology, 2006.
- [18] Lixing Zhu, MS Li, QH Wu, and L Jiang. Short-term natural gas demand prediction based on support vector regression with false neighbours filtered. *Energy*, 80:428–436, 2015.